ACS APPLIED MATERIALS & INTERFACES

LETTER

www.acsami.org

Enhanced Performance of Dye-Sensitized Solar Cells by Utilization of an External, Bifunctional Layer Consisting of Uniform β-$NaYF_4$:Er^{3+}/Yb^{3+} Nanoplatelets

Guo-Bin Shan, Hassane Assaaoudi, and George P. Demopoulos*

Department of Materials Engineering, McGill University, Montreal, PQ, H3A 2B2 Canada

Supporting Information

ABSTRACT: Uniform β-$NaYF_4$:Er^{3+}/Yb^{3+} hexagonal nanoplatelets were synthesized via a modified hydrothermal route, and the nanoplatelets were applied as an external, bifunctional layer in a novel DSC configuration consisting of only one internal TiO_2 transparent layer. Approximately 10% enhancements of photocurrent and overall DSC efficiency are demonstrated by the addition of the external layer, which exhibits two functions of light reflecting and near-infrared (NIR) light harvesting. The novel DSC configuration not only simplifies the DSC fabrication process but also eliminates charge recombination induced by the conducting up-converting nanocrystals when used internally thus opening the path for other more efficient up-converting nanocrystals to be designed and applied.

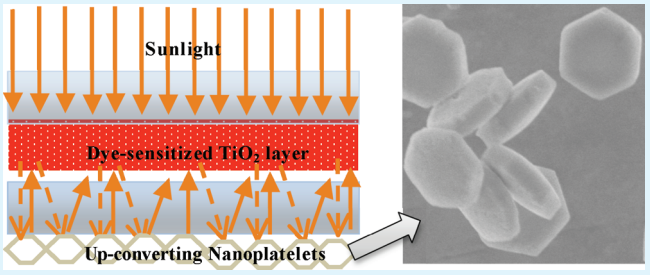

KEYWORDS: dye-sensitized solar cell, external layer, hydrothermal, nanoplatelets, $NaYF_4$:Er^{3+}/Yb^{3+}, up-conversion, reflection

1. INTRODUCTION

Dye-sensitized solar cells (DSCs) invented in 1991 use a dye to harvest sunlight and generate photocurrent.[1,2] Since then, tremendous progress in the field of the DSCs has been made because of their potential low-cost compared to the traditional silicon solar cells.[3] The DSC is typically a sandwich-structured solar cell consisting of substrate glass with transparent conducting oxides (TCO) layer, a few-μm-thick mesoporous TiO_2 film coated with a dye, an iodide/iodine (I_3^-/I^-) electrolyte, and Pt-coated TCO-glass used as a counter electrode. The sunlight harvesting by the TiO_2 surface-adsorbed dye can be improved by either introducing larger TiO_2 particles (200−1000 nm) in the transparent TiO_2 film of 15−30 nm-sized TiO_2 nanoparticles or printing them on top of the transparent TiO_2 film as a scattering layer.[4,5] These larger TiO_2 particles scatter light by multiple reflections, increasing their optical path length. As a result, the absorption of sunlight is enhanced and in turn photocurrent output is improved. The I_{sc} increases by as much as 16% by using 200−400 nm sized anatase particles as light-scattering centers.[4,6] Spherical voids can also act as light-scattering centers when introduced in the transparent TiO_2 film, enhancing the photovoltaic performance by 25%.[7] About 6-μm-thick scattering layers consisting of 500−1000 nm sized TiO_2, ZrO_2, or mixtures of the two in various proportions were placed on the top of the transparent TiO_2 films.[8,9] Amorphous Er^{3+} and Yb^{3+} codoped TiO_2 was also used as the scattering layer in DSCs contributing to an overall increase of 15.6% in efficiency.[10] In all these cell configurations, the scattering layer placed on top of the transparent nanocrystalline TiO_2 layer is an internal structural component; hence, we describe it as an internal light-scattering strategy.

An alternative strategy to improve light harvesting can be the utilization of an up-converting phosphor (UC), which transforms lower energy photons (>900 nm) into high-energy visible photons (<750 nm) that are absorbable by the dye.[11,12,20] One of the best known up-converter materials is β-$NaYF_4$:Er^{3+}/Yb^{3+} owing its up-conversion properties to Er^{3+} doping with Yb^{3+} codopant assisting in the energy transfer process.[20] For example, $NaYF_4$:Er^{3+} up-converting phosphors have been applied to silicon solar cells to obtain enhanced near-infrared (NIR) response.[13] An enhancement of 10 mA cm^{-2} was obtained under illumination with a 980 nm diode laser (10 mW) by applying $NaYF_4$:Yb^{3+}/Er^{3+} particles in amorphous silicon solar cells.[19] The same researchers commented recently that optimization of the synthesis of the up-conversion material, i.e., $NaYF_4$:Yb^{3+}/Er^{3+}, should be pursued to improve its response-an aspect addressed in this work.[20] $Y_3Al_5O_{12}$:Er^{3+}/Yb^{3+} has been used to convert NIR light to green light (~563 nm) for enhancing the NIR response of the DSCs.[18] Theoretical estimation shows about 5% increase of the energy conversion efficiency by adding the UC in silicon solar cells.[12] Recently, we reported on the use of a TiO_2/UC (made of Er^{3+}/Yb^{3+}-doped LaF_3) nanocomposite as (internal) part of the DSC structure in an effort to enhance light harvesting in the NIR region.[14] This configuration, however, proved, ineffective in delivering a higher photocurrent output because of apparent charge recombination at the UC/dye/electrolyte interfaces.

Received: May 1, 2011
Accepted: August 16, 2011
Published: August 16, 2011

Scheme 1. Schematic Configuration of the Novel DSC Device Consisting of One Internal TiO_2 Transparent Layer Plus an External Rear Layer of β-$NaYF_4$:Er^{3+}/Yb^{3+} Nanoplatelets

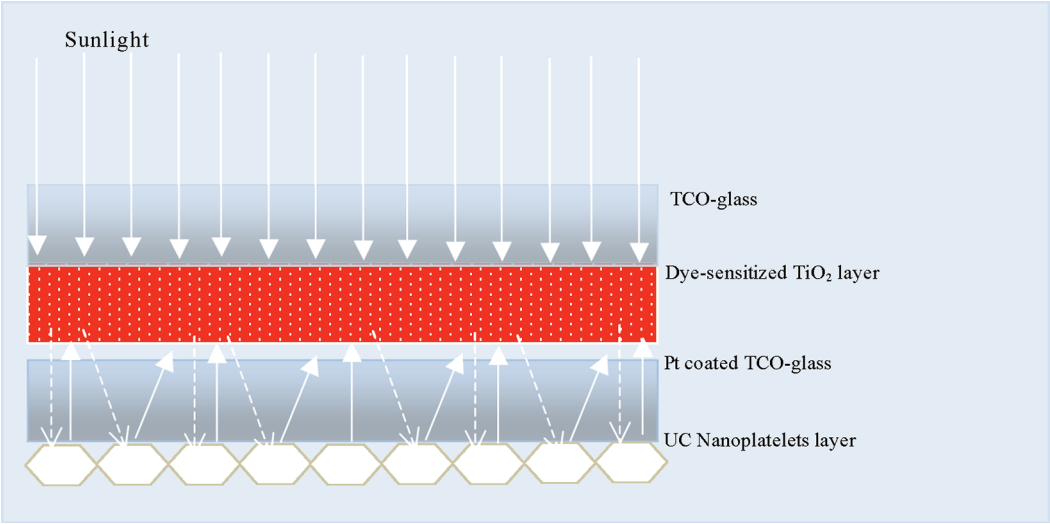

The present work reports, for the first time, on a new DSC structure configuration that consists of one internally TiO_2 transparent layer plus an external light-reflecting and NIR light harvesting bifunctional layer consisting of uniform β-$NaYF_4$:Er^{3+}/Yb^{3+} hexagonal nanoplatelets-an upconversion material morphology not investigated previously (Scheme 1).[20] The bifunctional layer is placed on the external side of the counter electrode. The advantage of this novel strategy is not only that simplifies DSC fabrication and provides two functions (light-reflection and up-conversion) but also does not affect the thickness of the internal transparent TiO_2 film, which is one of the critical factors affecting the overall efficiency of the DSCs, nor involves unnecessary dye loading. In this work, novel DSC devices comprising the internal transparent layer and the β-$NaYF_4$:Er^{3+}/Yb^{3+} nanoplatelet external layer are fabricated and analyzed. In particular, the ~10% enhancement of photocurrent and overall efficiency of the DSCs by the addition of this nanoplatelet-based external layer is demonstrated.

2. FABRICATION AND CHARACTERIZATION OF DYE-SENSITIZED SOLAR CELLS

The internal TiO_2 transparent layer DSC devices (DSCs) were fabricated as follows.[17] A transparent TiO_2 film on TCO glass (3-mm thickness, 13.5 ohms/sq., 81.4% of transmittance, Nippon Sheet Glass, Japan) was prepared by screen-printing a commercial TiO_2 paste (18-NT, Dyesol, Australia) followed by an annealing treatment and then sensitized with N719 dye (Dyesol, Australia). This N719-sensitized TiO_2 film/TCO glass was used as the working electrode of the DSCs. The counter electrode was Pt-deposited TCO-glass. A 25 μm-thickness sealant (Dyesol, Australia) was used as a spacer between two electrodes in order to seal them together under heating at 120 °C. The I_3^-/I^--based electrolyte (EL-HPE, Dyesol, Australia) was injected into the solar cell through a hole at the counter electrode side. The hole was sealed with a cover slide and the sealant to avoid leakage of the electrolyte solution. Fabrication of the novel DSCs with the external layer made of the β-$NaYF_4$:Er^{3+}/Yb^{3+} hexagonal nanoplatelets (E-DSCs): an ethanol suspension of the β-$NaYF_4$:Er^{3+}/Yb^{3+} hexagonal nanoplatelets (5 mg mL^{-1}) was deposited on a substrate followed by heating at 60 °C to remove the ethanol. This deposition process was repeated until a certain thickness of β-$NaYF_4$:Er^{3+}/Yb^{3+} film was formed. To completely remove any organic debris and internal water from the film, we subjected the latter to heat treatment. Finally, the film was placed on the rear side of the counter electrode of DSCs.

Photovoltaic measurements were made with a small area solar simulator (PV Measurements Inc.) equipped with an AM1.5G filter (PV Measurements Inc.). The power of the simulated light was calibrated to an overall intensity of 100 mW cm^2 by using a standard solar cell. I−V curves were obtained by applying an external photomask (0.4 × 0.4 cm^2) to the cell and measuring the generated photocurrent with a Keithley 2400 source meter. For each device a minimum of three measurements were made from which average values were obtained and reported. The model of the 980 nm fiber laser was L3-PTX98 (JDS Uniphase), and the fiber core diameter was 105 μm. Power supply for the laser was obtained from a GW INSTEK unit (model PSP-2010).

3. RESULTS AND DISCUSSION

3.1. Configuration of DSC Devices. In this work, we applied an external layer consisting of β-$NaYF_4$:Er^{3+}/Yb^{3+} hexagonal nanoplatelets (Figure 1) on the rear side of the one internal-layer DSC (Scheme 1). The β-$NaYF_4$:Er^{3+}/Yb^{3+} nanoplatelets were synthesized via a modified hydrothermal route (see the Supporting Information).[21] Under the excitation of 980 nm light, green (peak at 510−570 nm) and red (peak at 640−680 nm) emissions from the β-$NaYF_4$:Er^{3+}/Yb^{3+} nanoplatelet-made film were observed, respectively (Figure 2). The green emission corresponds to excitation routes from excited state $^2H_{11/2}$, $^4F_{7/2}$, and $^4S_{3/2}$ to the ground state $^4I_{15/2}$ of Er^{3+} under the 980 nm irradiation; and the red one emitted from excited state $^4F_{9/2}$ to the $^4I_{15/2}$.[15,16] Further, it is noted that the intensity of the green emission is much higher than that of the red emission according to the area values of the emission peak and the color observation

with naked eyes. The stronger green emission indicates that the nanoplatelets can be an excellent candidate for NIR light harvesting in DSCs because the N-719 sensitizer in the DSCs efficiently absorbs the green light converted from the NIR light.[14] In addition to its up-conversion properties, the film made from the β-$NaYF_4$ nanoplatelets is white, and hence is capable of total light-reflection.

To investigate the dual NIR light up-conversion and light reflection effect of the external layer on the photovoltaic performance of the DSC, two types of DSCs were fabricated: (1) a control DSC consisting of a dye N719-sensitized transparent TiO_2 film on TCO glass as working electrode, Pt-coated TCO glass as the counter electrode, and I^-/I_3^- liquid electrolyte; and (2) an experimental device with the external β-$NaYF_4$:Er^{3+}/Yb^{3+} hexagonal nanoplatelet-comprising layer (E-DSC).

3.2. Effect of TiO_2-Layer Thickness on Performance of E-DSCs. Because the thickness of the TiO_2 layer is one of the factors affecting short-circuit current density (I_{sc}) and overall DSC efficiency (η),[4,6,16,22] a series of devices (with and without the inclusion of the external UC layer) with different TiO_2 film thickness were fabricated. The hexagon size and the thickness of the nanoplatelets used in Sections 3.1−3.3 were about 0.8 μm × 0.2 μm, respectively (Figure 1). The photovoltaic characteristics of these devices under AM1.5 G sunlight as well as under 980 nm light are shown in Table 1. In both types of devices, 14 ± 0.5 μm thickness was determined to be the optimum for the transparent TiO_2 layer. The internal scattering layer (typically 4−5 μm thickness) in conventional DSCs might become a barrier to electron/charge or electrolyte diffusion.[4] Such diffusion problem is removed in the novel DSC configuration. Both I_{sc} and η are clearly enhanced by the addition of the β-$NaYF_4$:Er^{3+}/Yb^{3+} rear layer. No evident change of fill factor (FF) and the open-circuit voltage (V_{oc}) happens with the introduction of the β-$NaYF_4$:Er^{3+}/Yb^{3+} layer as the latter is placed externally to the dye-sensitized photoanode/electrolyte system.

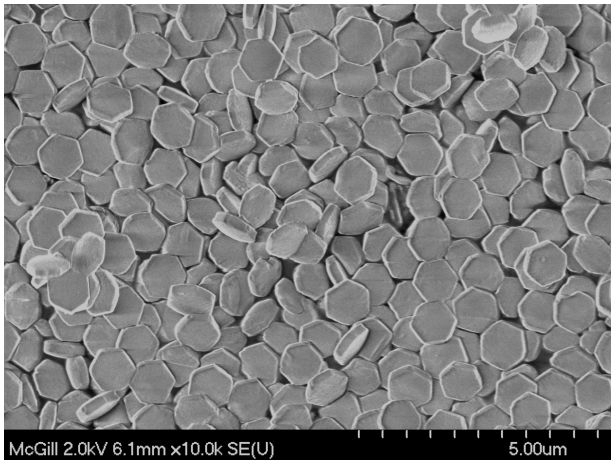

Figure 1. SEM images of the β-$NaYF_4$:Er^{3+}/Yb^{3+} nanoplatelets.

3.3. Effect of the β-$NaYF_4$:Er^{3+}/Yb^{3+} Nanoplatelet External Layer on E-DSC Performance. At the optimum TiO_2 layer thickness, the photovoltaic characteristics of the standard DSC were, V_{oc} = 0.634 V, I_{sc} = 16.45 mA cm^{-2}, FF = 0.66 and η = 6.94%. Upon the addition of the β-$NaYF_4$:Er^{3+}/Yb^{3+} rear layer, the I_{sc} and η were enhanced to 17.91 mA cm^{-2} and η = 7.36% but as mentioned FF and V_{oc} remained the same. The photovoltaic response of the E-DSCs is shown in Table 1 and Figure 3. Under this NIR light source (2.4 W power), 0.25−0.40 V of V_{oc} and 0.030−0.050 mA of I_{sc} were obtained in the E-DSCs, respectively clearly confirming the upconverting function of the external β-$NaYF_4$:Er^{3+}/Yb^{3+} rear layer. Hence, compared with the control DSC device, the improvement of both the photocurrent density (I_{sc}, up to 11.1% increase) and the overall efficiency (η, up to 10.2% increase) in the E-DSC device is attributed to combining light reflective action and NIR light-harversting (upconversion) properties of the β-$NaYF_4$:Er^{3+}/Yb^{3+} nanoplatelet-made rear layer.

In a previous work, we proposed NIR sunlight harvesting in DSCs by inserting a LaF_3:Er^{3+}/Yb^{3+}-TiO_2 nanocomposite layer between the transparent TiO_2 layer and the scattering TiO_2 layer.[14] That configuration proved ineffective, however, because the LaF_3:

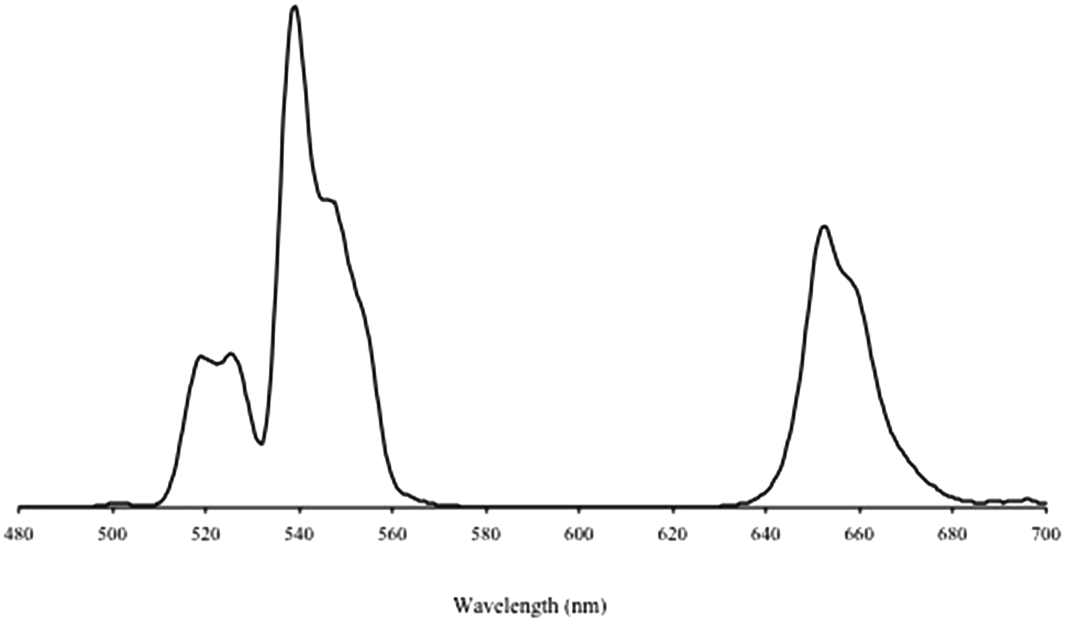

Figure 2. Up-conversion fluorescence spectra of the β-$NaYF_4$:Er^{3+}/Yb^{3+} nanoplatelets layer.

Table 1. $I-V$ Parameters for the DSC and E-DSC Devices under AM 1.5G Filtered Spectral Illumination at an Intensity of 100 mW cm^{-2} or a 980 nm Fiber Laser with an Operating Output Power of 2.4 W

	AM1.5 G solar simulator										980 nm fiber laser	
	V_{oc} (V)		I_{sc} (mA cm^{-2})			FF		η (%)				
thickness (μm)	DSCs	E-DSCs	DSCs	E-DSCs	increase (%)	DSCs	E-DSCs	DSCs	E-DSCs	increase (%)	V_{oc} (V)	I (mA)
5 ± 0.5	0.624	0.629	14.07	15.32	8.9	0.62	0.62	5.48	5.95	8.6	0.33	0.030
7 ± 0.5	0.629	0.634	15.07	16.42	8.9	0.64	0.64	6.06	6.68	10.2	0.39	0.050
9 ± 0.5	0.634	0.634	15.50	16.77	8.2	0.64	0.65	6.30	6.87	9.1	0.38	0.040
12 ± 0.5	0.634	0.634	15.92	17.69	11.1	0.66	0.65	6.67	7.25	8.7	0.31	0.043
14 ± 0.5	0.634	0.639	16.45	17.91	8.9	0.66	0.64	6.94	7.36	6.1	0.29	0.040
16 ± 0.5	0.664	0.664	14.93	16.22	8.6	0.68	0.65	6.72	7.05	4.9	0.26	0.044
18 ± 0.5	0.624	0.629	14.06	15.13	7.6	0.64	0.63	5.62	5.94	5.6	0.25	0.049

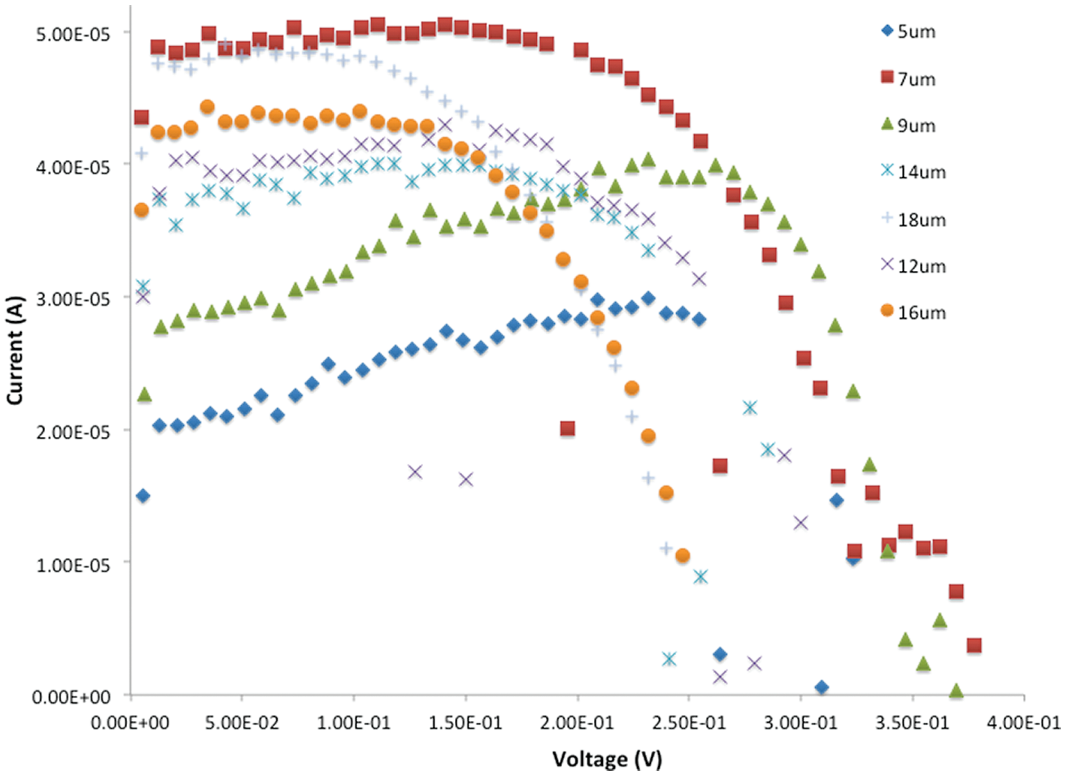

Figure 3. $I-V$ characteristics of E-DSCs with different internal layer thickness under illumination with a 2.4W power 980 nm laser.

Er^{3+}/Yb^{3+} nanocrystals acted as charge recombination centers causing loss of the photocurrent generated by the NIR light harvesting. The photocurrent of the present configuration produced by the 980 nm laser is much higher (~38% increase) than that in the previous work. Similar results were obtained in the present work when the layer of β-$NaYF_4$:Er^{3+}/Yb^{3+} upconversion nanoplatelets was inserted in the interior of the cell on top of the transparent TiO_2 layer and in contact with the electrolyte. In this case the photovoltaic performance (for a cell with the standard 14 ± 0.5 μm TiO_2 film thickness) dropped to V_{oc} = 0.624 V, I_{sc} = 14.07 mA cm^{-2}, FF = 0.62 and η = 5.48%. Hence the external β-$NaYF_4$:Er^{3+}/Yb^{3+} nanoplatelet layer as described in this work greatly overcomes the charge recombination drawback while at the same time offers an easily fabricated and elegant structure.

3.4. Effect of Er^{3+}/Yb^{3+} Dopants on E-DSC Performance. According to the above presented results, the external layer consisting of β-$NaYF_4$:Er^{3+},Yb^{3+} nanoplatelets yields ~10% DSC efficiency and photocurrent enhancement attributed to its dual functions of light reflecting and NIR up-converting. In order to differentiate the contribution of the up-converting effect, E-DSCs were fabricated of whose the external layers consisted of β-$NaYF_4$ nanoplatelets not only doped with Er^{3+}/Yb^{3+} but also without them. As mentioned in the introduction it is the dopants that are responsible for the up-converson of NIR light to visible light.[20] For this series of tests new β-$NaYF_4$ nanoplatelets were synthesized under the same conditions with and without the upconverting Er^{3+},Yb^{3+} dopants. In the experiment, we used two different-sized platelets, i.e., 2.0 μm × 0.5 μm, and 0.75 μm × 0.2 μm, for fabricating the external layers. These

Table 2. Photovoltaic Response of E-DSCs (internal TiO_2 layer 6−7 μm thick) with and without Er^{3+}/Yb^{3+} Doping of the β-$NaYF_4$ Nanopletelets (NP), under AM 1.5G Filtered Spectral Illumination at an Intensity of 100 mW cm^{-2}

device	average NP size (μm)	dopant Er^{3+}/Yb^{3+}	V_{oc} (V)	I_{sc} (mA cm^{-2})	increase (%)	FF	η (%)	increase (%)
A			0.60	11.12		0.62	4.05	
AB0	2.0 × 0.5	without	0.61	12.54	12.7	0.61	4.45	9.9
AB1		with	0.62	12.83	15.3	0.62	4.47	10.4
AC0	0.75 × 0.2	without	0.60	12.67	13.9	0.60	4.33	6.90
AC1		with	0.60	12.84	15.4	0.60	4.38	8.15

can be seen in the supporting material of this paper (see Figures S4.1 and 2 in the Supporting Information). Their photovoltaic data are presented in Table 2.

As per data of Table 2, once more the addition of the external layer can be seen to yield enhanced photovoltaic performance, namely an increase up to 15.4% for I_{sc} and up to 10.4% for cell efficiency. Closer evaluation of the data shown in Table 2 reveals that the observed enhancements are predominantly due to the light reflecting action of the β-$NaYF_4$ nanolatelet-based external layer. The up-conversion contribution of the Er^{3+},Yb^{3+} dopants by difference is estimated at ∼1% both in terms of photocurrent and conversion efficiency. This is a relatively significant result as it demonstrates for the first time the upconversion enhancing effect of Er^{3+},Yb^{3+} under full sun illumination as opposed to previous "proof-of-principle" tests employing 980 nm laser illumination only.[18,19] Apparently the choice and crystal design of the host material plays an important role in this context with the β-$NaYF_4$ hexagonal nanolatelets reported in this work performing better than, for example, $Y_3Al_5O_{12}$: Er^{3+}/Yb^{3+} or TiO_2: Er^{3+}/Yb^{3+} tried in DSCs or poorly described β-$NaYF_4$:Er^{3+}, Yb^{3+} particles used in an amorphous silicon solar cell.[10,18,19] Further optimization of the up-conversion material, however, as pointed out recently,[20] is required to render up-conversion a viable option in solar cell fabrication.

4. CONCLUSIONS

A novel DSC configuration consisting of an internal transparent anatase (TiO_2) layer plus an external bifunctional layer was proposed, which can simultaneously reflect light and utilize near-infrared (NIR) light thus having the advantages of simplified DSC fabrication and enhanced light to current efficiency and photocurrent output. The external layer is optimally made from uniform β-$NaYF_4$:Er^{3+}/Yb^{3+} hexagonal nanoplatelets synthesized by a simple hydrothermal route.

■ ASSOCIATED CONTENT

Supporting Information. Materials, methods, and characterization information, including additional figures (PDF). This material is available free of charge via the Internet at http://pubs.acs.org.

■ AUTHOR INFORMATION

Corresponding Author
*E-mail: george.demopoulos@mcgill.ca.

■ ACKNOWLEDGMENT

The project is funded through the strategic research grant program of NSERC (the Natural Sciences and Engineering Research Council of Canada). The authors express their appreciation to Dr. Mark P. Andrews and Ph.D. student Mr. Timothy Gonzalez of McGill's Department of Chemistry for the use of their PTI fluorescence spectrophotometer and the 980 nm fiber laser.

■ REFERENCES

(1) O'Regan, B.; Grätzel, M. *Nature* **1991**, *353*, 737–740.
(2) Grätzel, M. *Acc. Chem. Res.* **2009**, *42*, 1788–1798.
(3) Hagfeldt, A.; Boschloo, G.; Sun, L.; Kloo, L.; Pettersson, H. *Chem. Rev.* **2010**, *110*, 6595–6663.
(4) Ito, S.; Murakami, T. N.; Comte, P.; Liska, P.; Grätzel, C.; Nazeeruddin, M. K.; Grätzel, M. *Thin Solid Films* **2008**, *516*, 4613–4619.
(5) Zhang, Z.; Ito, S.; O'Regan, B.; Kuang, D.; Zakeeruddin, S. M.; Liska, P.; Charvet, R.; Comte, P.; Nazeeruddin, Md-K.; Péchy, P.; Humphry-Baker, R.; Koyanagi, T.; Mizuno, T.; Grätzel, M. *Z. Phys. Chem.* **2007**, *221*, 319–327.
(6) Rothenberger, G.; Comte, P.; Grätzel., M. *Solar Energy Mater. Solar Cells* **1999**, *58*, 321–336.
(7) Hore, S.; Nitz, P.; Vetter, C.; Prahl, C.; Niggemann, M.; Kern, R. *Chem. Commun.* **2005**, 2011–2013.
(8) Huang, F.; Chen, D.; Zhang, X. L.; Caruso, R. A.; Cheng, Y. B. *Adv. Funct. Mater.* **2010**, *20*, 1301–1305.
(9) Hore, S.; Vetter, C.; Kerna, R.; Smit, A. H. *Solar Energy Mater. Solar Cells* **2006**, *90*, 1176–1188.
(10) Han, C. H.; Lee, H. S.; Lee, K.; Han, S. D.; Sing, I. *Bull. Korean Chem. Soc.* **2009**, *30*, 219–223.
(11) Trupke, T.; Green, M. A.; Würfel, P. *J. Appl. Phys.* **2002**, *92*, 4117–4122.
(12) Badescu, V.; Badescu, A. M. *Renewable Energy* **2009**, *34*, 1538–1544.
(13) Shalav, A.; Richards, B. S.; Trupke, T.; Krämer, K. W.; Güdel, H. U. *App. Phys. Lett.* **2005**, *86*, 013505.
(14) Shan, G. B.; Demopoulos, G. P. *Adv. Mater.* **2010**, *22*, 4373–4377.
(15) Shan, G. B.; Andrews, M. P.; Gonzalez, T.; Djeghelian, H. *Mater. Lett.* **2008**, *62*, 4187–4190.
(16) Suyver, J. F.; Grimm, J.; van Veen, M. K.; Biner, D.; Krämer, K. W.; Güdel, H. U. *J. Lumin.* **2006**, *117*, 1–12.
(17) Charbonneau, C.; Lee, K. E.; Shan, G. B.; Gomez, M. A.; Gauvin, R.; Demopoulos, G. P. *Electrochem. Solid-State Lett.* **2010**, *13*, H257–H260.
(18) Liu, M.; Lu, Y.; Xie, Z. B.; Chow, G. M. *Solar Energy Mater. Solar Cells* **2011**, *95*, 800–803.
(19) de Wild, J.; Meijerink, A.; Rath, J. K.; van Sark, W. G. J. H. M.; Schropp, R. E. I. *Solar Energy Mater. Solar Cells* **2010**, *94*, 1919–1922.
(20) de Wild, J.; Meijerink, A.; Rath, J. K.; van Sark, W. G. J. H. M.; Schropp, R. E. I. *Energy Environ. Sci.* **2011**, DOI: 10.1039/c1ee01659h.
(21) Li, C.; Yang, J.; Yang, P.; Zhang, X.; Lian, H.; Lin, J. *Cryst. Growth Des.* **2008**, *8*, 923–929.
(22) Charbonneau, C.; Gauvin, R.; Demopoulos, G. P. *J. Electrochem. Soc.* **2011**, *158*, H224–H23.